DOI 10.1007/s11106-016-9764-5
Powder Metallurgy and Metal Ceramics, Vol. 54, Nos. 11-12, March, 2016 (Russian Original Vol. 54, Nos. 11-12, Nov.-Dec., 2015)

CALORIMETRIC STUDY OF THE $La_2Hf_2O_7$ HEAT CAPACITY IN THE RANGE 57–302 K

A. R. Kopan',[1,2] M. P. Gorbachuk,[1] S. M. Lakiza,[1] and Ya. S. Tishchenko[1]

UDC 536.631:546.654′546.832′546.21

The heat capacity of $La_2Hf_2O_7$ has been studied in the range 57–302 K by adiabatic calorimetry. The heat capacity C_p of lanthanum hafnate changes monotonically and there are no anomalies. The values of heat capacity, entropy, enthalpy, and reduced Gibbs energy have been determined in standard conditions: C_p° (298.15 K) = 229.39 ± 0.92 J · mol^{-1} · K^{-1}, S^o (298.15 K) = 246.9 ± 2 J × × mol^{-1} · K^{-1}, Φ° (298.15 K) = 114.76 ± 1.72 J · mol^{-1} · K^{-1}, and H^o (298.15 K)–H^o (0 K) = 39403 ± ± 197 J · mol^{-1}. In the series of isostructural $La_2Zr_2O_7 \rightarrow La_2Hf_2O_7$ compounds, atomic oscillation frequency in the lattice decreases and low-temperature heat capacity increases with greater mass of oscillator atoms from Zr to Hf.

***Keywords**: thermodynamics, heat capacity, enthalpy, entropy, reduced Gibbs energy, lanthanum hafnate.*

INTRODUCTION

Compounds of composition $Ln_2Hf_2O_7$ (where Ln = La–Tb) form in the HfO_2–Ln_2O_3 systems and have cubic structure of pyrochlore $NaCaTa_2O_6(OH, F)$ [1, 2]. The constitution, thermal stability, chemical inertness, and low thermal conductivity of pyrohafnates make them promising materials for refractory oxide ceramics, high-temperature composites, and thermal-barrier coatings [3, 4]. The oxygen-ion conductivity of these compounds indicates that they can be applied as electrolytes for solid-oxide fuel cells (SOFCs) and gas sensors and as membranes for oxygen evolution [4, 5]. There are published data on the suitability of hafnates $Ln_2Hf_2O_7$ for developing matrices for storage of radioactive waste because, first, they are inert to radiation and, second, can form solid solutions with actinide oxides [6].

Recent experiments conducted to examine the heat capacity and magnetic susceptibility of rare-earth metal hafnates [7, 8] show that magnetics with a pyrochlore lattice remain disordered over a wide range below the Curie–Weiss temperature (10 K). The strong geometric frustration in these compounds, making conventional ordering impossible, leads to complete destruction of long-range ordering and formation of a new collective paramagnetic state like that of a spin fluid, possessing unique thermodynamics in the magnetic field. There are prospects for using the magnetocaloric effect, observed in [7, 8], in cryogenic applications.

[1]Frantsevich Institute for Problems of Materials Science, National Academy of Sciences of Ukraine, Kiev, Ukraine.

[2]To whom correspondence should be addressed; e-mail: allakop@ipms.kiev.ua.

Translated from Poroshkovaya Metallurgiya, Vol. 54, Nos. 11–12 (506), pp. 81–90, 2015. Original article submitted November 12, 2014.

To optimize the processes of obtaining new materials with desired properties, reliable data on thermodynamic characteristics of the compounds involved are required. Hence, to choose materials for the design of equipment and to determine their economic feasibility, heat capacity needs to be taken into account. The HfO_2–Ln_2O_3–Al_2O_3 phase diagrams cannot be successfully studied without understanding the thermodynamic properties of their components and phases.

ANALYSIS OF RESEARCH EFFORTS

Information on the thermodynamic properties of light rare-earth metal hafnates is scarce [7–12]. According to the literature review, research into the thermodynamic characteristics of $Ln_2Hf_2O_7$ was initiated [10] by scientists of the Indira Gandhi Centre for Atomic Research (Kalpakkam, India). In the referenced study, increase in the enthalpy of $La_2Hf_2O_7$, $Eu_2Hf_2O_7$, and $Gd_2Hf_2O_7$ was measured by the mixing technique in the range 1000–1740 K and the thermodynamic functions (enthalpy, heat capacity, entropy, reduced Gibbs energy) of these compounds were determined in a range from 300 to 1800 K. The samples were also subjected to X-ray diffraction, but [10] does not provide the results. The standard deviation of the enthalpies of $La_2Hf_2O_7$, $Eu_2Hf_2O_7$, and $Gd_2Hf_2O_7$ in the above temperature range was 2.96, 2.22, and 1.46%.

To study the magnetic properties of pyrochlores, the heat capacity of $Gd_2Hf_2O_7$ was examined in [7] in the range 0.4–6 K with an accuracy of ~5%. At T_C = 0.771 K, the heat capacity curve has a sharp peak, resulting from long-range magnetic ordering (second-order phase transition). The peak corresponds to ~17 $J \cdot mol^{-1} \cdot K^{-1}$, which agrees to within 18% with the value calculated with the mean-field approximation for the second-order phase transition at S = 7/2. The magnetic entropy $S(T)$ for $Gd_2Hf_2O_7$ was also evaluated in [7] by extrapolating the heat capacities C_p° (T) to T = 0 K.

The heat capacity of $Pr_2Hf_2O_7$ was measured in the range 0–25 K [8]. There is a wide maximum at 2–10 K on the temperature dependence of C_p° for hafnate praseodymium. To ascertain the causes behind the abnormal behavior of heat capacity, the purity of the $Pr_2Hf_2O_7$ samples was tried to be improved. For this purpose, they were synthesized by different techniques: from oxides (ceramic technique), from hydroxides (chemical technique), annealing in hydrogen, and annealing at higher temperatures. It was revealed [8] that, first, synthesis of $Pr_2Hf_2O_7$ from hydroxides followed by annealing in hydrogen did not improve the purity, while its annealing at high temperatures (to 1700°C) required the removal of most admixtures and, second, the total heat capacity C_p changed insignificantly, the lattice component being subtracted, at low temperatures when there was a wide maximum. The authors believe that this is indicative of strong geometrical frustration, unusual ordering.

Of interest today is to study the thermodynamic characteristics of phase transformations [1, 11], formation [1], and evaporation [12] of rare-earth metal hafnates of composition $Ln_2Hf_2O_7$. There are no published data on the low-temperature heat capacity of $La_2Hf_2O_7$. Therefore, our objective is to examine the constant-pressure heat capacity of $La_2Hf_2O_7$ in the range 60–300 K.

EXPERIMENTAL PROCEDURE

The La_2O_3–HfO_2 system was studied in the range 1200–2820°C in [13]. Compound $La_2Hf_2O_7$ (LH_2) forming in this system melts congruently at 2420°C. It has a wide homogeneity range, varying with temperature. The homogeneity range of the LH_2 phase is 25.5–37.5% La_2O_3 at a eutectic temperature of 2330°C, 23–38% La_2O_3 at a eutectic temperature of 2070°C, and 29–37% La_2O_3 at 1900°C. The La_2O_3–HfO_2 phase diagram is shown in Fig. 1.

The test samples were produced by thermal decomposition of a nitrate mixture (chemical technique). The starting substances were HfO_2 containing 99.95% of the base material (GFO-2 grade, Donetsk Chemical Reagent Plant) and La_2O_3 (ultrahigh purity, LaoD grade, as per OST 48-194–81). Stoichiometric amounts of the La_2O_3 and $HfO(NO_3)_2$ powders were dissolved in nitric acid diluted with water in a one-to-one ratio. The solutions were mixed and subjected to reverse coprecipitation. The precipitate was washed with distilled water and dried in air, and the granules were ground.

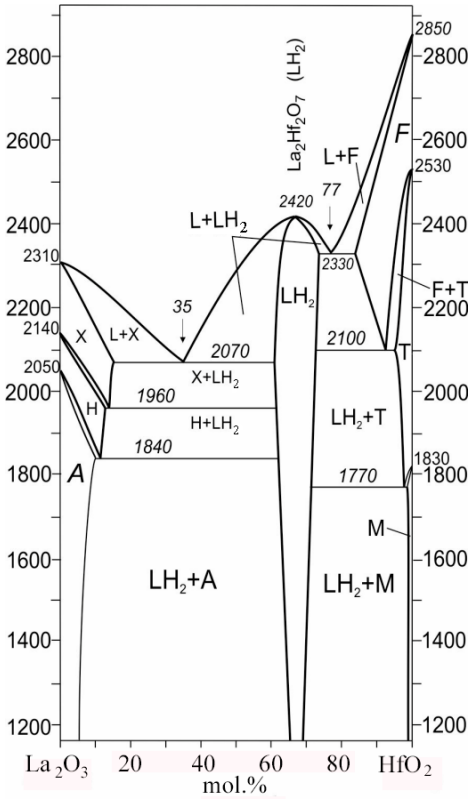

Fig. 1. The La_2O_3–HfO_2 phase diagram

The powder was pressed to make pellets 8 mm in diameter and 5–8 mm in height to be then annealed at 1250°C for 5 h to remove organics and for the mixture components to react with each other. The latter is especially important since free La_2O_3 should be bound in $La_2Hf_2O_7$ because otherwise it will react with atmospheric moisture to form $La(OH)_3$ and, consequently, destroy the pellets.

The samples for analysis were molten in a focused beam of a solar furnace with a precise sun-tracking device in air because of high temperature (2420°C) and congruent melting of lanthanum hafnate. The molten samples were examined with X-ray diffraction at room temperature using a DRON-1.5 diffractometer (Cu-K_α radiation, Ni filter) with a scan rate of 1/4–4 °C/min in the range 2θ = 15–100°. The intensity of lines was evaluated visually on a ten-point scale or in percentage from the relative height of the diffraction peaks (Fig. 2). The lattice parameters of cubic phases were calculated with the least-squares method employing the LATTICE software, with an error not higher than 0.0004 nm. X-Ray Powder Diffraction File cards were used for phase analysis of the samples.

The $La_2Hf_2O_7$ lattice parameter was a = 1.0775 nm, which agrees with [13, 14]. According to [13], the $La_2Hf_2O_7$ lattice parameters within the homogeneity range 62–73 mol.% HfO_2 vary from 1.0785 to 1.0719 nm. This

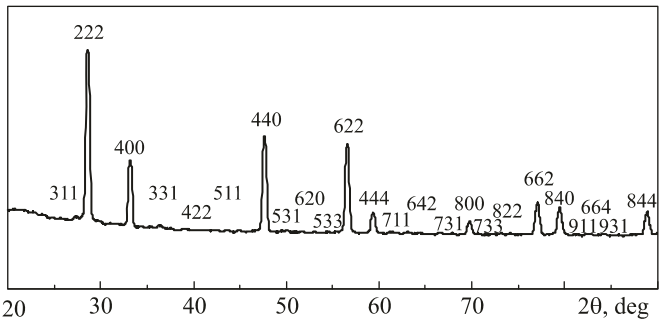

Fig. 2. X-ray diffraction pattern of the $La_2Hf_2O_7$ sample

allowed us to determine the composition of the molten samples, being 63.7 mol.% HfO_2. This composition falls within the homogeneity range with a small shift (3 mol.%) toward excess La_2O_3. Petrographic analysis revealed a single-phase material with refractive index $n = 2.02$.

The heat capacity of $La_2Hf_2O_7$ was studied adiabatically with heat being supplied periodically at a low-temperature calorimeter (UNTO) designed at the *Dalstandart* Scientific & Production Association (Russia) [15]. The UNTO calorimeter with a volume of 10 cm^3 was partially upgraded as follows: a capsule 3.8 mm in diameter and 20 mm in height was soldered in at the calorimeter bottom. The calorimeter was qualified using a standard thermodynamic α-Al_2O_3 sample with a weight of 10.7987 g according to the procedure described in [16]. The measurement error was no higher than 0.4% in the range 60–300 K.

RESULTS AND DISCUSSION

The constant-pressure heat capacity of $La_2Hf_2O_7$ has been studied for the first time in the range 57.31–302.18 K using a 20.1698 g sample. The results were processed with three software programs [17] to: smooth the experimental data, extrapolate the temperature dependence of heat capacity to 0 K, and calculate the main thermodynamic functions (enthalpy, entropy, reduced Gibbs energy). The smoothed heat capacities of $La_2Hf_2O_7$ in the range 60–300 K are summarized in Table 1.

TABLE 1. Thermodynamic Functions of $La_2Hf_2O_7$

T, K	C_p° (T), J · K^{-1} · mol^{-1}		S^o (T), J · K^{-1} · mol^{-1}	$H^o(T) - H^o(0)$, J · mol^{-1}	Φ^o (T), J · K^{-1} · mol^{-1}
	Smoothed	Calculated			
10	–	1.70	1.70	8.52	0.86
20	–	3.80	3.46	34.96	1.70
30	–	9.98	5.94	98.30	2.66
40	–	22.36	10.40	255.98	4.00
50	–	37.58	17.00	554.76	5.90
60	52.70	52.88	25.20	1007.54	8.42
70	67.47	67.28	34.46	1609.20	11.46
80	80.93	80.64	44.32	2349.68	14.96
90	93.13	93.02	54.54	3218.82	18.78
100	104.08	104.52	64.94	4207.30	22.88
110	114.79	115.20	75.42	5306.60	27.18
120	124.86	125.12	85.88	6508.84	31.64
130	134.38	134.32	96.26	7806.64	36.20
140	143.20	142.88	106.52	9193.18	40.86
150	151.20	150.82	116.66	10662.16	45.58
160	158.60	158.22	126.64	12207.82	50.34
170	165.47	165.14	136.44	13825.00	55.12
180	171.98	171.60	146.06	15509.02	59.90
190	177.85	177.68	155.50	17255.76	64.68
200	183.22	183.42	164.76	19061.60	69.46
210	188.42	188.86	173.84	20923.30	74.22
220	193.44	194.04	182.76	22838.08	78.94
230	198.32	199.00	191.48	24803.48	83.64
240	203.14	203.74	200.06	26817.32	88.32
250	207.88	208.32	208.46	28877.76	92.96
260	212.51	212.72	216.72	30983.08	97.56
270	217.08	217.00	224.84	33131.84	102.12
280	221.45	221.16	232.80	35322.70	106.64
290	225.70	225.18	240.64	37554.48	111.14
298.15	229.39	228.40	246.92	39402.92	114.76
300	230.48	229.13	248.32	39826.15	115.58

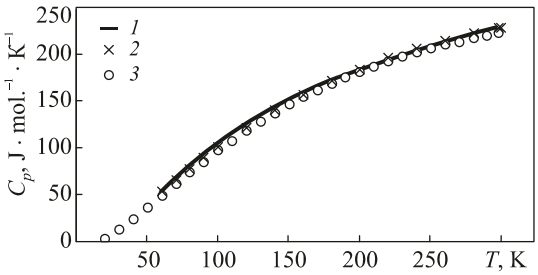

Fig. 3. Heat capacity of ternary isostructural $La_2Hf_2O_7$ (*1*), $La_2Hf_2O_7$ (calculated with NKR) (*2*), and $La_2Zr_2O_7$ [18] (*3*)

The root-mean-square deviation of experimental C_p° from the averaged values was 0.24%. The technique proposed in [17] to extrapolate the heat capacities to 0 K allowed us to calculate the enthalpy $H^o(T) - H^o(0)$, entropy $S^o(T)$, and reduced Gibbs energy $\Phi^o(T)$ of lanthanum hafnate up to 300 K with errors no higher than 0.5, 0.8, and 1.5%, respectively. The root-mean-square deviation of calculated C_p from the smoothed values was 0.23%. The $H^o(T) - H^o(0)$, $S^o(T)$, and $\Phi^o(T)$ values of $La_2Hf_2O_7$ for the range 0–300 K and standard conditions are provided in Table 1.

We compared the experimental heat capacities of $La_2Hf_2O_7$ in the range 57–302 K with the C_p° values (Fig. 3, curve *2*) obtained for this compound with the Neumann–Kopp rule (NKR) and with experimental C_p° for isostructural lanthanum zirconate $La_2Zr_2O_7$ (Fig. 3, curve *3*) [18]. In the entire temperature range, the heat capacity of $La_2Hf_2O_7$ increases monotonically, no anomalies being observed (Fig. 3, curve *1*).

The NKR calculations are known [19] to be the simplest universal method to evaluate C_p° (298.15 K) and temperature dependence of the heat capacity for complex oxides. The main advantage of NKR is that there are experimental data on the temperature dependence of heat capacity for most simple oxides. This method was used to calculate the molar heat capacity C_p° of $La_2Hf_2O_7$ in the range 50–300 K as a sum of the heat capacities of oxides forming this compound as follows:

$$C_p^\circ(La_2Hf_2O_7) = C_p^\circ(La_2O_3) + 2C_p^\circ(HfO_2). \quad (1)$$

The dependences $C_p(T)$ La_2O_3 and HfO_2 were borrowed from [20] and [21], respectively. The data reported in [20, 22] on the heat capacity of lanthanum oxide agree well in a wide temperature range and are approximately 1% lower than Westrum's results [23]. Experimental C_p° for HfO_2 [24] were processed with the least-squares method in [21] to obtain the following equation:

$$C_p(\text{J} \cdot \text{mol}^{-1} \cdot \text{K}^{-1}) = -9.7516 + 0.3779T - 0.00048T^2 + \frac{1421.87}{T^2}. \quad (2)$$

Figure 3 shows that the experimental heat capacities of $La_2Hf_2O_7$ and those evaluated by Eq. (1) are close. A comparative analysis indicates that the maximum difference between the experimental and calculated values is 3.8% at 80 K, which is no more than the error of determining C_p° with NKR (~5%). The compared values differ by 0.2 to 1.5% at 150–300 K; this is lower than in the range 70–140 K. It should be noted that the inaccuracy in determining the heat capacity (~3%) often causes significant errors in calculations of phase equilibria and other thermodynamic properties. Hence, reliable experimental data on the heat capacity of compounds are required to calculate the latter.

The heat capacity of $La_2Hf_2O_7$ systematically exceeds C_p° of $La_2Zr_2O_7$ [18], which is illustrated in Fig. 3. The greatest difference in C_p° of these compounds is observed at 70 K (~9%), and C_p° gradually decreases to 1–3% in the range 150–298.15 K. The lattice component of the insulator heat capacity is crucial in the temperature range

studied. The distinctions between C_p° for $La_2Hf_2O_7$ and $La_2Zr_2O_7$ may be due to different energies of chemical bonding in these compounds and different masses of their particles.

To characterize interatomic bonds in the lattice, whose degree and nature primarily determine the strength of any body, we have compared the published data on basic structural and some physical properties of lanthanum hafnate and lanthanum zirconate (Table 2).

According to [25], La—O and B—O bonds (where B is Hf or Zr) are covalent with an insignificant ionic contribution. With reducing distance between the atoms, the covalent contribution increases in the crystal; hence, B—O bonds are stronger than La—O bonds (Table 2). At the same time, the ionic contribution in B—O bonds increases in transfer from $La_2Hf_2O_7$ to $La_2Zr_2O_7$. To evaluate the degree of ionic/covalent bonds in the compounds, the Mulliken population analysis was applied in [6] to calculate the overlap population of La—O and B—O bonds. The results (Table 2) agree with the previous conclusions and confirm that the covalent contribution in lanthanum hafnate bonds is greater (higher numerical value of overlap population) than in isostructural zirconate.

According to [25], the modulus of elasticity increases with a smaller lattice parameter: the evaluated bulk modulus of elasticity for $La_2Hf_2O_7$ is higher than for $La_2Zr_2O_7$ (Table 2). The deformation and fracture of materials are known to be opposed by interatomic bond forces; hence, bonds in the $La_2Hf_2O_7$ phase are stronger than in $La_2Zr_2O_7$.

Table 2 shows that the melting enthalpy and temperature of lanthanum hafnate are higher and the minimum total energy is lower than those of lanthanum zirconate. This means that the energy of interaction between lattice atoms increases in the $La_2Zr_2O_7 \rightarrow La_2Hf_2O_7$ series. The lattice thus becomes more rigid, leading to higher oscillation frequency and lower energy of the atoms.

On the other hand, when mass m of the oscillator atoms increases, the mass of Hf becoming almost two times as high as that of Zr, the oscillation period $\tau = 2\pi\sqrt{m/k}$ (where k is the oscillator coefficient of elasticity) becomes greater and atomic oscillation frequency thus lower. According to quantum theory [27], low-frequency oscillations (acoustic oscillations) are major contributors to the lattice heat capacity at low temperatures. This

TABLE 2. Comparison of Some Lattice Parameters, Chemical Bonds, and Physical Properties of Isostructural Lanthanum Hafnate and Lanthanum Zirconate

Parameter	$La_2Hf_2O_7$	$La_2Zr_2O_7$
Lattice parameter a, nm:		
calculation [25]	1.0754	1.0848
experiment [26]	1.0776	1.0805
our data [18]	1.0775	1.0804
Interatomic spacing, nm:		
B (Hf, Zr)—O	0.2147 / 0.2091*	0.2105 / 0.2114
La—O	0.2555 / 0.2630	0.2635 / 0.2645
La—O'	0.2333 / 0.2328	0.2339 / 0.2348
O—O	0.2740 / 0.2770	0.2780 / 0.2791
O—O'	0.3050 / 0.3162	0.3166 / 0.3178
Orbital overlap population [6]:		
La—O	0.041	0.037
B (Hf, Zr)—O	0.096	0.027
Heat capacity C_p(298.15 K), J · mol^{-1} · K^{-1}	229.39	223.05 [18]
Melting point T_{melt} [11], K	2653 ± 10	2553 ± 10
Melting enthalpy ΔH [11], kJ · mol^{-1}	~350	~280
Bulk modulus of elasticity B (calculation [25]), GPa	174.925	166.918
Minimum total energy (calculation [25]), eV	–597163	–345555

* Experimental [26]/calculated [25] interatomic spacing.

explains the higher heat capacity of the $La_2Hf_2O_7$ lattice as compared to the $La_2Zr_2O_7$ phase. The wavelengths corresponding to low-frequency oscillations are most likely greater than interatomic spacing. Hence, features of the crystalline structure are not sensitive to and have almost no influence on the lattice heat capacity in the temperature range studied.

CONCLUSIONS

Adiabatic calorimetry has been employed to study the constant-pressure heat capacity of $La_2Hf_2O_7$ in the range 57–302 K. It is shown that C_p° of lanthanum hafnate changes monotonically without any anomalies.

The heat capacity, entropy, reduced Gibbs energy, and enthalpy of the $La_2Hf_2O_7$ phase in standard conditions have been determined for the first time, and temperature dependences of the main thermodynamic functions of the $La_2Hf_2O_7$ phase have been obtained for the range 10–300 K.

In the series of isostructural $La_2Zr_2O_7 \rightarrow La_2Hf_2O_7$ compounds, atomic oscillation frequency in the lattice decreases and low-temperature heat capacity increases with greater mass of oscillator atoms from Zr to Hf.

REFERENCES

1. S. V. Ushakov and A. Navrotsky, "Energetics of defect fluorite and pyrochlore phases in lanthanum and gadolinium hafnates," *J. Am. Ceram. Soc.*, **90**, No. 4, 1171–1176 (2007).
2. A. S. Povarennykh, *Crystallochemical Classification of Minerals* [in Russian], Naukova Dumka, Kyiv (1966), p. 547.
3. V. G. Sevastyanov, E. P. Simonenko N. A. Ignatov, et al., "Synthesis and study of the thermal stability of superfine refractory lanthanum and neodymium zirconates and hafnates for thermal-barrier coatings," *Kompos. Nanostruct.*, No. 1, 50–58 (2009).
4. A. V. Shlyakhtina, *Synthesis and Properties of Oxygen-Ion Conducting Compounds of Rare-Earth Pyrochlore Family* [in Russian], Author's Abstract of ScD Thesis, 02.00.21, Moscow (2010), p. 46.
5. A. V. Shlyakhtina and L. I. Shcherbakova, "New solid electrolytes of the pyrochlore family," *Rus. J. Electrochem.*, **48**, No. 1, 1–25 (2012).
6. G. R. Lumpkin, M. Pruneda, S. Rios, et al., "Nature of the chemical bond and prediction of radiation tolerance in pyrochlore and defect fluorite compounds," *J. Solid State Chem.*, **180**, 1512–1518 (2007).
7. A. M. Durand, R. Klavins, and L. R. Corruccini, "Heat capacity of the frustrated magnetic pyrochlores $Gd_2Zr_2O_7$ and $Gd_2Hf_2O_7$," *J. Phys. Condens. Matter*, **20**, 235208–235212 (2008).
8. H. Craig, "Magnetic frustration and phase purity in pyrochlore materials $Pr_2Zr_2O_7$, $Pr_2Hf_2O_7$, and $Tb_2Hf_2O_7$," *US Davis Undergraduate Res. J.*, **12**, 23–41 (2009).
9. V. K. Anand, A. K. Bera, J. Xu, et al., "Observation of long range magnetic ordering in pyrohafnate $Nd_2Hf_2O_7$: a neutron diffraction study," *Phys. Rev. B*, **92**, No. 18, 184418 (2015).
10. R. Babu and K. Nagarajan, "Calorimetric measurements on rare earth pyrohafnates $RE_2Hf_2O_7$ (RE = La, Eu, Gd)," *J. Alloys Compd.*, **265**, 137–139 (1998).
11. S. V. Ushakov, S. P. Maram, A. Navrotsky, et al., "Study of $La_2Zr_2O_7$ and $La_2Hf_2O_7$ melting by thermal analysis and X-ray diffraction," in: *Proc. Conf. Honolulu PRiME-2012* (October 7–12, 2012, Honolulu, Hawaii, USA), Honolulu (2012), p. 2329.
12. V. G. Sevastyanov, E. P. Simonenko, D. V. Sevastyanov, et al., "Synthesis, vaporization, and thermodynamics of ultrafine $Nd_2Hf_2O_7$ powders," *Russ. J. Neorg. Chem.*, **58**, No. 1, 3–10 (2013).
13. A. V. Shevchenko, L. M. Lopato, and Z. A. Zaitseva, "Interaction of HfO_2 with lanthanum, praseodymium, and neodymium oxides at high temperatures," *Izv. AN SSSR. Neorg. Mater.*, **20**, No. 9, 1530–1534 (1984).
14. A. W. Sleight, "New ternary oxides of mercury with the pyrochlore structure," *Inorg. Chem.*, **7**, No. 9, 1704–1708 (1968).

15. A. S. Bolgar, N. P. Gorbachuk, A. V. Blinder, et al., "Thermodynamic characteristics of lanthanum mono- and disilicide at low temperatures," *Zh. Fiz. Khim.*, **70**, No. 7, 1185–1189 (1996).
16. *Certification Procedure for Units Designed to Determine Specific Heat Capacity and Specific Enthalpy of Solid Materials* [in Russian], Izd. Standartov, Moscow (1978), p. 19.
17. V. P. Turov, A. S. Bolgar, A. V. Blinder, et al., *Heat Capacity of Zirconium Diboride and Molybdenum Monoboride at Low Temperatures* [in Russian], Dep. VINITI No. 3657-V86, June 20, 1986, Inst. Probl. Materialoved. AN USSR, Kyiv (1986), p. 14.
18. M. Bolech, E. H. P. Cordfunke, A. C. G. van Genderen, et al., "The heat capacity and derived thermodynamic functions of $La_2Zr_2O_7$ and $Ce_2Zr_2O_7$ from 4 to 1000 K," *J. Phys. Chem. Solids*, **58**, No. 3, 433–439 (1997).
19. J. Leitner, P. Chuchvalec, D. Sedmidubsky, et al., "Estimation of heat capacities of solid mixed oxides," *Thermochimica Acta*, **395**, 27–46 (2003).
20. H. W. Goldstein, E. F. Neilson, P. N. Walsh, et al., "The heat capacities of yttrium oxide (Y_2O_3), lanthanum oxide (La_2O_3), and neodymium oxide (Nd_2O_3) from 16 to 300 K," *J. Phys. Chem.*, **63**, 1445–1449 (1959).
21. *Thermophysical Properties Database of Materials for Light Water Reactors and Heavy Water Reactors*, Final Report of a Coordinated Research Project 1999–2005, International Atomic Energy Agency, Vienna (2006), p. 397.
22. E. G. King, W. W. Weller, and L. B. Pankratz, *Thermodynamic Data for Lanthanum Sesquioxide*, Bureau of Mines, U. S. Department of the Interior, Washington (1961), No. 5857, pp. 1–6.
23. B. H. Justice and E. F. Westrum, "Thermophysical properties of lanthanide oxides. I. Heat capacities, thermodynamic properties, and some energy levels of lanthanum (III) and neodymium (III) oxides from 5 to 350 K," *J. Phys. Chem.*, **67**, 339–345 (1963).
24. S. S. Todd, "Heat capacities at low temperatures and entropies at 298.16 K of hafnium dioxide and hafnium tetrachloride," *J. Am. Chem. Soc.*, **75**, No. 12, 3035–3036 (1953).
25. R. Terki, H. Feraoun, G. Bertrand, et al., "Full potential linearized augmented plane wave investigations of structural and electronic properties of pyrochlore systems," *J. Appl. Phys.*, **96**, No. 11, 6482–6487 (2004).
26. M. A. Subramanian, G. Aravamudan, and G. V. Subba Rao, "Oxide pyrochlores−a review progress in solid state chemistry," *Prog. Solid State Chem.*, **15**, No. 2, 55–143 (1983).
27. S. M. Skuratov, V. P. Kolesov, and A. F. Vorob'ev, *Thermochemistry* [in Ukrainian], Izd. Mosk. Gos. Univ., Moscow (1966), Part 2, p. 434.